# Modeling coupled bending, axial, and torsional vibrations of a CANDU fuel rod subjected to multiple frictional contact constraints

M. Fadaee and S. D. Yu Department of Mechanical and Industrial Engineering Ryerson University, Toronto, Ontario, Canada M5B 2K3

**ABSTRACT** - In this paper, a finite element based dynamic model is presented for bending, axial, and torsional vibrations of an outer CANDU fuel element subjected to multiple unilateral frictional contact (MUFC) constraints. The Bozzak-Newmark relaxation-integration scheme is used to discretize the equations of motion in the time domain. At a time step, equations of state of the fuel element with MUFC constraints reduce to a linear complementarity problem (LCP). Results are compared with those available in the literature. Good agreement is achieved. The 2D sliding and stiction motion of a fuel element at points of contact is obtained for harmonic excitations.

#### Introduction

In a CANDU fuel channel, the heavy water coolant flows through a string of fuel bundles and brings out the heat generated by fuel elements for steam production. To understand the complex behaviour of flow-induced vibration of the fuel string, accurate and reliable models must be developed to capture the elasto-rigid motions of fuel elements subjected to non-smooth unilateral frictional contact constraints at multiple locations. The friction between the outer fuel element's bearing pads and the pressure tube is two-dimensional. An individual fuel element moves with the fuel bundle in a rigid body manner in the closely packed spaces of a fuel channel, and deforms as a slender structure in the form of bending, axial and torsional deformations.

Yetisir and Fisher [1] investigated the effect of turbulence excitation on fretting wear between fuel element bearing pads and pressure tube. Hassan and Rogers [2] studied vibration of a fuel element by applying several frictional models to investigate the effect of tube-support clearance and preload. Xu et al. [3] investigated bending vibration of a single fuel element subjected to frictionless contact by means of beam finite element method and the Wilson- $\theta$  method. Recently Yu and Fadaee [4] presented a finite element model for bending, axial, and torsional free vibrations of a straight beam using three-node higher-order mixed finite element. As of today, the effects of 2D friction on fuel element vibration are not investigated.

Considering the complex geometry of a fuel element and the non-smooth constraints, a valid vibration model of a fuel element should be based on the finite element method. Practically fuel elements experience small rigid displacements and small elastic displacements due to the limited available spaces inside a fuel channel. This allows for the use of linear theories (linear relationships between stresses and strains, and linear relationships between strains and displacement gradients), and more importantly consideration of rigid body displacements within the framework of the structural finite elements. This makes it possible to develop a feasible fuel string vibration model for simulating fuel string fretting and fretting induced component wear in a fuel channel.

In this paper, the discrete equations of motion of an unconstrained CANDU fuel element are derived by means of the Lagrange equations. An implicit incremental displacement Bozzak-Newmark scheme is then employed to seek a numerical solution in the time domain for predicting harmonically excited bending, axial and torsional vibrations of an outer fuel element subjected to 2D friction and unilateral contact constraints with the pressure tube. To be able to effectively handle the two types of the non-smooth constraints - 2D friction and unilateral contact, the equations of system states are formulated in terms of the incremental displacements. In handling the multiple unilateral frictional constraints at a time step, the sub-structuring method is used to eliminate all interior DOF's [5]. The coupled gap equations in the directions of all probable contact points and the their associated frictional forces in the two tangential directions (axial and circumferential) are reduced, through variable transformations and an auxiliary incremental displacement variable, to a linear complementarity problem (LCP) for which a solution can be obtained using the Lemke algorithm. At each time step, the incremental displacement vectors are resolved into the tangential and normal directions of motion. Base on Coulomb's law of friction, the frictional force acts in the direction opposite to the true direction of motion or tendency of motion. In the proposed approach, the direction angle of the frictional force is estimated based on the velocities at the end of the previous time step. For small time steps, the proposed scheme yields satisfactory results without iterations. The contact forces in the radial direction and the frictional force in the tangential direction along with the sliding velocities are computed for each paired contact. These parameters can be used to assess the material loss of the pressure tube.

# 1. Equation of Motion of a Single Fuel Element

Assume that a fuel bundle is concentrically placed inside a straight pressure tube. The origin of the bundle coordinates oxyz is at the bundle geometric centre with three axes oriented as shown in Figure 1. The origin of the coordinates  $(oxyz)_i$  for fuel element i is at the midspan with the three axes oriented along the radial, tangential and axial directions. The coordinates for the centre fuel element are identical to the bundle coordinates.

Although the dominating dynamic response of a fuel element appears to be bending, the axial vibration and torsional vibration are also present when the effects of bearing pads and endplates are considered. A CANDU-6 fuel element is a very slender structure with a length-to-diameter ratio of about 38. Under normal operating conditions, the sheath is expected to be fully collapsed onto the pellets. The sheath along with the pellets form a monolithic compound beam. As a result, we decided to employ the classical theories for all three types of vibrations of a fuel element.

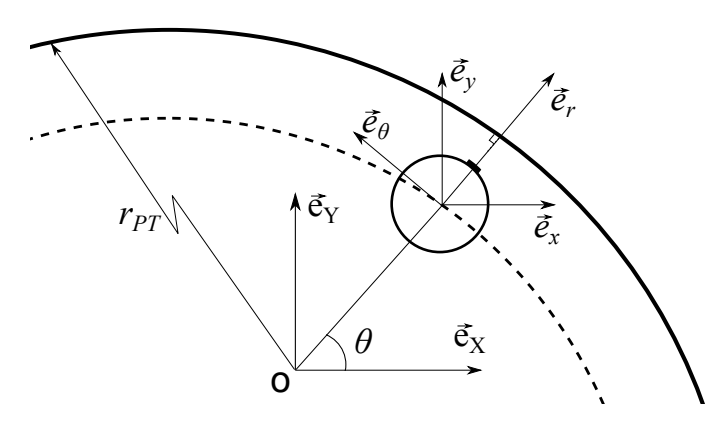


Figure 1 Cross sectional view of an outer most fuel element and pressure tube

According to the classical theories of bending, axial stretching, and torsion, the displacements of a material point in a fuel element are related to four one-dimensional field variables as described in [4],

$$u_{x}(x, y, z, t) = u(z, t) - y\emptyset(z, t)$$

$$u_{y}(x, y, z, t) = v(z, t) + x\emptyset(z, t)$$

$$u_{z}(x, y, z, t) = w(z, t) - x\frac{\partial u(z, t)}{\partial z} - y\frac{\partial v(z, t)}{\partial z}$$
(1)

where,  $u_x$ ,  $u_y$  and  $u_z$  are the displacements of a material point (x,y,z) in the three coordinate directions, respectively; u and v are the lateral displacements associated with bending; w is the axial displacement;  $\emptyset$  is the angle of twist associated with torsion. Under dynamic loads, a fuel element subjected to ordinary and unilateral frictional contact constraints can exhibit very complex vibrational behavior. Using the finite element method and the Lagrange equations, we may obtain the following equations of motion in terms of the generalized coordinates as

$$[M]{\ddot{q}} + [C]{\dot{q}} + [K]{q} = {Q} + {Q_f} - {Q_c}$$
(2)

where [M], [K] and [C] are the mass, stiffness and damping matrices, respectively;  $\{Q\}$  is the excitation force vector;  $\{Q_f\}$  is the frictional force vector; and  $\{Q_c\}$  is the unilateral contact forces;  $\{q\}$  is the generalized displacement vector.

# 2. Handling 2D Friction and Unilateral Contact

A fuel element is subjected to unilateral contact and 2D frictional constraints. The contact forces and the friction forces are not known a priori. A solution to the governing differential equations cannot be obtained in a straightforward manner. To seek a solution in the time domain, the entire time interval of interest,  $t \in [t_0, t_f]$ , is divided into n small and equal time intervals:  $[t_0, t_1], [t_1, t_2], ..., [t_i, t_{i+1}], ..., [t_{n-1}, t_n]$ , where  $t_i = t_0 + ih$ , i = 0,1,2,...,n, h is the uniform time step. It should be noted that no temporal convergence has been investigated for this work. If

the state of the dynamical system at  $t = t_i$  is determined, the state of the system at  $t = t_{i+1}$  may be found by solving the following differential equations

$$(1 + \alpha)[M]\{\ddot{q}\}_{i+1} - \alpha[M]\{\ddot{q}\}_{i+1} + [C]\{\dot{q}\}_{i+1} + [K]\{q\}_{i+1}$$

$$= \{Q\}_{i+1} + \{Q_f\}_{i+1} - \{Q_c\}_{i+1}$$
(3)

where  $\alpha$  is the relaxation factor. By using Newmark integration scheme, Eq. (3) could be written as

$$[k^*]\{\Delta q\}_{i+1} = \{Q^*\}_{i+1} + \{Q_f\}_{i+1} - \{Q_c\}_{i+1}$$
(4)

where

$$[k^*] = (1+\alpha)\frac{1}{\beta h^2}[m] + \frac{\gamma}{\beta h}[c] + [k],$$

$$\{Q^*\}_{i+1} = \{Q\}_{i+1} + [m]\left(\frac{1+\alpha}{\beta h^2}\{q\}_i + \frac{1+\alpha}{\beta h}\{\dot{q}\}_i + \left(\frac{1}{2\beta} - 1 + \frac{\alpha}{2\beta}\right)\{\ddot{q}\}_i\right)$$

$$+ [c]\left(\frac{\gamma}{\beta h}\{q\}_i + \left(\frac{\gamma}{\beta} - 1\right)\{\dot{q}\}_i + \left(\frac{\gamma}{2\beta} - 1\right)h\{\ddot{q}\}_i\right) - [k^*]\{q\}_i$$

$$\{\Delta q\}_{i+1} = \{q\}_{i+1} - \{q\}_i$$

where  $\gamma$  and  $\beta$  are Newmark coefficients. In this study, the following values are used,  $\alpha = 0.1, \beta = 0.5, \gamma = 0.6$ .

# 2.1 Sub-structuring and Transformations

Since the interior displacements are not involved explicitly in the contact formulations, the generalized force due to contact associated with interior DOF's are zero. To eliminate the interior DOF's, we use the following transformation

$$[\Delta q]_{i+1} = [T] \begin{Bmatrix} \Delta q_o \\ \Delta q_j \end{Bmatrix}_{i+1} \tag{5}$$

where subscript "o" refer to interior and "j" refers to interfacial DOF's. Substituting Eq. (5) into Eq. (4) and pre-multiplying the so-obtained equations by  $[T]^T$  we obtain

$$\begin{bmatrix} k_{oo} & k_{oj} \\ k_{jo} & k_{jj} \end{bmatrix} \begin{Bmatrix} \Delta q_o \\ \Delta q_j \end{Bmatrix}_{i+1} = \begin{Bmatrix} Q^*_o \\ Q^*_j \end{Bmatrix}_{i+1} + \begin{Bmatrix} 0 \\ Q_f \end{Bmatrix}_{i+1} - \begin{Bmatrix} 0 \\ Q_c \end{Bmatrix}_{i+1}$$
 (6)

We can now eliminate the interior displacements by representing them as a function of interfacial DOF's,

$$\{\Delta q_o\}_{i+1} = k_{oo}^{-1} \left( \{Q^*_o\}_{i+1} - k_{oj} \{\Delta q_j\}_{i+1} \right) \tag{7}$$

Substitute Eq. (7) into Eq. (6) and re-write the equilibrium equation only considering interfacial DOF's,

$$k_1^* \left\{ \Delta q_j \right\}_{i+1} = k_2^* \left\{ Q_o^* \right\}_{i+1} + \left\{ Q_f^* \right\}_{i+1} + \left\{ Q_f \right\}_{i+1} - \left\{ Q_c \right\}_{i+1}$$
 (8)

where,  $k_1^* = k_{jj} - k_{jo} k_{oo}^{-1} k_{oj}$  And  $k_2^* = -k_{jo} k_{oo}^{-1}$ .

To formulate the gap equations, the incremental displacement vector are first expressed in terms of the radial, circumferential and axial components. The transformation may be written as (see Figure 1)

When contact occurs, the circumferential and axial displacements of the fuel element at the point of contact are two-dimensional motion. By choosing a small time step, we may assume that these two incremental displacements are in a 2D plane on the inner surface of pressure tube. However the trajectory of the point of contact on this 2D plane is not known a priori. The axial and circumferential incremental displacements,  $\Delta w$  and  $\Delta u_{\theta}$ , may be resolved in terms of tangential and normal directions as shown in Figure 2.

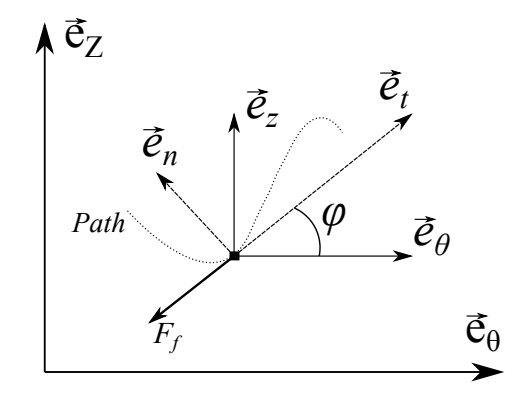


Figure 2 Transformation of incremental displacement

This may be written as

The two transformations may be written together as

$$\begin{cases}
\Delta u \\
\Delta v \\
\Delta w
\end{cases} = \begin{bmatrix}
\cos \theta & -\sin \theta & 0 \\
\sin \theta & \cos \theta & 0 \\
0 & 0 & 1
\end{bmatrix} \begin{bmatrix}
1 & 0 & 0 \\
0 & \cos \varphi & -\sin \varphi \\
0 & \sin \varphi & \cos \varphi
\end{bmatrix} \begin{Bmatrix}
\Delta u_r \\
\Delta u_t \\
\Delta u_n
\end{Bmatrix} = [A] \begin{Bmatrix}
\Delta u_r \\
\Delta u_t \\
\Delta u_n
\end{Bmatrix} \tag{11}$$

Substitute Eq. (11) into Eq. (8) and pre-multiply by  $A^{-1}$ ,

Holiday-Inn Waterfront Hotel Kingston, Ontario, Canada, 2013 September 15-18

$$A^{-1}k_{1}^{*}A\left\{\Delta q_{j}^{*}\right\}_{i+1}$$

$$=A^{-1}k_{2}^{*}\{Q_{o}^{*}\}_{i+1} + A^{-1}\left\{Q_{j}^{*}\right\}_{i+1} + A^{-1}\left\{Q_{f}\right\}_{i+1} - A^{-1}\left\{Q_{c}\right\}_{i+1}$$

$$(12)$$

After some rearrangement, we obtain

$$k_{r1}^* \left\{ \Delta q_j^* \right\}_{i+1} = \left\{ Q^{**} \right\}_{i+1} - \left\{ Q_c^* \right\}_{i+1} + \left\{ Q_f^* \right\}_{i+1} \tag{13}$$

where,

$$\{Q^{**}\}_{i+1} = k_{r2}^* \{Q^*_{o}\}_{i+1} + A^{-1} \left\{Q^*_{j}\right\}_{i+1}, \qquad k_{r1}^* = A^{-1} k_1^* A, \qquad k_{r2}^* = A^{-1} k_2^*,$$

Vectors in Eq. (13) are given below,

$$\left\{ \Delta q_j^* \right\} = \left\{ \begin{matrix} \Delta u_r \\ \Delta u_t \\ \Delta u_n \end{matrix} \right\}, \qquad \left\{ Q^{**} \right\} = \left\{ \begin{matrix} Q_r^{**} \\ Q_t^{**} \\ Q_n^{**} \end{matrix} \right\}, \qquad \left\{ Q_c^* \right\} = \left\{ \begin{matrix} F_c \\ 0 \\ 0 \end{matrix} \right\}, \qquad \left\{ Q_f^* \right\} = \left\{ \begin{matrix} 0 \\ F_f \\ 0 \end{matrix} \right\}$$

where  $F_f$  and  $F_c$  indicate the frictional and contact force respectively. Notice that the frictional force in the direction normal to the direction of motion is zero. Now from Eq. (13), the incremental displacement in the normal direction may be represented as a function of the radial and tangential incremental displacement as

$$\Delta u_{n_{i+1}} = k_{r_{133}}^{*}^{-1} (Q_{n_{i+1}}^{**} - k_{r_{131}}^{*} \Delta u_{r_{i+1}} - k_{r_{132}}^{*} \Delta u_{t_{i+1}})$$
(14)

Substitute Eq. (14) into Eq. (13)

$$k_{r1}^{*} \begin{cases} \Delta u_{r} \\ \Delta u_{t} \\ k_{r1_{33}}^{*-1} (Q_{n_{i+1}}^{**} - k_{r1_{31}}^{*} \Delta u_{r_{i+1}} - k_{r1_{32}}^{*} \Delta u_{t_{i+1}}) \end{cases}_{i+1} = \begin{cases} Q_{r}^{**} \\ Q_{t}^{**} \\ Q_{n}^{**} \end{cases}_{i+1} + \begin{cases} F_{c} \\ F_{f} \\ 0 \end{cases}_{i+1}$$

$$(15)$$

Now first and second row in Eq. (15) could be written as

$$\overline{K}\{\Delta U\}_{i+1} + \{\overline{Q}\}_{i+1} = -\{\overline{Q}_c\}_{i+1} + \{\overline{Q}_f\}_{i+1}$$
(16)

Where,

$$\begin{split} \overline{K} &= \begin{bmatrix} k_{r1_{11}}^* - k_{r1_{13}}^* k_{r1_{33}}^{*}^{-1} k_{r1_{31}}^* & k_{r1_{12}}^* - k_{r1_{13}}^* k_{r1_{33}}^{*}^{-1} k_{r1_{32}}^{*} \\ k_{r1_{21}}^* - k_{r1_{23}}^* k_{r1_{33}}^{*}^{-1} k_{r1_{31}}^* & k_{r1_{22}}^* - k_{r1_{23}}^* k_{r1_{33}}^{*}^{-1} k_{r1_{32}}^{*} \end{bmatrix}, \quad \{\Delta U\}_{i+1} = \begin{Bmatrix} \Delta u_r \\ \Delta u_t \end{Bmatrix}_{i+1}, \\ \{ \overline{Q} \}_{i+1} &= \begin{Bmatrix} k_{r1_{13}}^* k_{r1_{33}}^{*} - k_{r1_{23}}^{*} k_{r1_{33}}^{*} - k_{r1_{33}}^{*} - k_{r1_{32}}^{*} k_{r1_{33}}^{*} - k_{r1_{32}}^{*} \end{bmatrix}, \quad \{ \overline{Q}_c \}_{i+1} = \begin{Bmatrix} C_c \\ 0 \end{Bmatrix}_{i+1}, \\ \{ \overline{Q}_f \}_{i+1} &= \begin{Bmatrix} 0 \\ F_f \end{Bmatrix}_{i+1}, \end{split}$$

# 2.2 Handling 2D Friction

According to Coulomb's law of friction, the frictional force is applied from the pressure tube to the node of contact on the fuel element opposite in direction to the motion and proportional to the normal force between two surfaces. In the normal direction to the contacting surfaces, the following equation of equilibrium hold true

$$\{P\}_{i+1} = \{N\}_{i+1} \tag{17}$$

where  $\{P\}_{i+1}$  is the summation of all external normal forces applied on that node of contact at  $t_{i+1}$  and  $\{N\}_{i+1}$  is the collective normal forces acting on the node of contact from the pressure tube. Multiplying Eq. (17) by  $\mu$ , coefficient of friction we will obtain

$$\mu\{N\}_{i+1} - \mu\{P\}_{i+1} = \{0\} \tag{18}$$

In this paper, the kinetic coefficient of friction is used for both stiction and sliding states. Four different scenarios are possible for the motion of the contact node at fuel element on the pressure tube, forward slip, stick with the tendency of motion in forward, stick with the tendency of moving backward and backward slip. In each possible state of motion frictional force may be represented as

- 1) Forward slip:  $\Delta u_{t_{i+1}} > 0$ ,  $(F_f)_{i+1} = -(\mu N)_{i+1}$
- 2) Forward stiction:  $\Delta u_{t_{i+1}} = 0$ ,  $-(\mu N)_{i+1} \le (F_f)_{i+1} \le 0$
- 3) Backward stiction:  $\Delta u_{t_{i+1}} = 0$ ,  $0 \le (F_f)_{i+1} \le (\mu N)_{i+1}$  (19)
- 4) Backward slip:  $\Delta u_{t_{i+1}} < 0$ ,  $(F_f)_{i+1} = (\mu N)_{i+1}$

States 1 and 2 in Eq. (19) represent the motion or tendency of motion in the tangential direction where  $\Delta u_{t_{i+1}} \ge 0$ , and states 3 and 4 represent the motion or tendency of motion in the negative tangential coordinate direction where  $\Delta u_{t_{i+1}} \le 0$ . For the states 1 and 2, we have

$$(\mu N)_{i+1} + (F_f)_{i+1} \ge 0 \tag{20}$$

For this state we would like to introduce following two new variables,

$$(\widehat{\Delta u_t})_{i+1} = \sup \left( \Delta u_{t_{i+1}}, 0 \right) \tag{21}$$

$$(\hat{s})_{i+1} = (\mu N)_{i+1} + (F_f)_{i+1} \tag{22}$$

where sup is the supremum of a set of variables,  $(\widehat{\Delta u_t})_{i+1}$  is the value of the incremental displacement if it is moving in positive direction and  $(\hat{s})_{i+1}$  is the value of the slack force. It could be verified that  $(\widehat{\Delta u_t})_{i+1}$  and  $(\hat{s})_{i+1}$  are non-negative and satisfy the complementary condition, which could be written as

$$\widehat{\Delta u_t} \ge 0, \qquad \widehat{s} \ge 0, \qquad \widehat{\Delta u_t}.\,\widehat{s} = 0$$
 (23)

Now for states 3 and 4 in Eq. (19), which are describing the motion or tendency of motion of the mass in negative tangent coordinate,  $\widehat{\Delta u_t} \leq 0$ , friction force is pointing toward positive tangent direction. According to the Coulomb's law of friction we may write,

Kingston, Ontario, Canada, 2013 September 15-18

$$(\mu N)_{i+1} - (F_f)_{i+1} \ge 0 \tag{24}$$

We introduce following two new variables,

$$(\widetilde{\Delta u_t})_{i+1} = \sup\left(-\Delta u_{t_{i+1}}, 0\right) \tag{25}$$

$$(\check{s})_{i+1} = (\mu N)_{i+1} - (F_f)_{i+1} \tag{26}$$

Again  $(\Delta u_t)_{i+1}$  and  $(\delta)_{i+1}$  are complementary to each other and the state of frictional interaction may be written as

$$\widetilde{\Delta u_t} \ge 0, \quad \check{s} \ge 0, \quad \widetilde{\Delta u_t}.\,\check{s} = 0$$
(27)

It can be verified that the incremental displacement in tangent direction could be written in terms of supremum variables as

$$\Delta u_t = \widehat{\Delta u_t} - \widecheck{\Delta u_t} \tag{28}$$

Write incremental displacements in terms of supremum variables in Eq. (16),

$$\overline{K}\{\widehat{\Delta U} - \widecheck{\Delta U}\}_{i+1} + \{\overline{Q}\}_{i+1} = \{Q_{c,r}\}_{i+1} + \{Q_{f,r}\}_{i+1}$$
(29)

Add Eq. (29) with Eq. (18) and subtract Eq. (29) from Eq. (18),

$$\overline{K}\{\widehat{\Delta U} - \widehat{\Delta U}\}_{i+1} + \{\overline{Q}\}_{i+1} = -\{Q_{c,r}\}_{i+1} + \{Q_{f,r}\}_{i+1} + \{\mu N\}_{i+1} - \{\mu P\}_{i+1}$$
(30)

$$-\overline{K}\{\widehat{\Delta U} - \widecheck{\Delta U}\}_{i+1} - \{\overline{Q}\}_{i+1} = \{Q_{c,r}\}_{i+1} - \{Q_{f,r}\}_{i+1} + \{\mu N\}_{i+1} - \{\mu P\}_{i+1}$$
(31)

Substitute Eq. (22) and (26) into Eq. (30) and (31),

$$\overline{K} \{ \Delta \overline{U} - \Delta \overline{U} \}_{i+1} + \{ \overline{Q} \}_{i+1} = -\{ Q_{c,r} \}_{i+1} + \{ \hat{s} \}_{i+1} - \{ \mu P \}_{i+1}$$
(32)

$$-\overline{K}\{\widehat{\Delta U} - \widecheck{\Delta U}\}_{i+1} - \{\overline{Q}\}_{i+1} = \{Q_{c,r}\}_{i+1} + \{\check{s}\}_{i+1} - \{\mu P\}_{i+1}$$
(33)

The contact force from pressure tube acting on fuel element is modelled as a gap activated spring. The contact force will present only when the initial gap is consumed. An auxiliary coordinate y introduced to represent the position of the spring end plate. If the stiffness of the gap activated spring is K equation of equilibrium at time  $t_{i+1}$  may be written as

$$Ky_{i+1} = F_{c_{i+1}} (34)$$

Considering Figure 1, the gap in the radial direction at time  $t_{i+1}$  may be written as

$$g_{i+1} = y_{i+1} - u_{r_{i+1}} + \Delta \tag{35}$$

where  $\Delta$  is the initial gap, from Eq. (35) we may obtain

$$y_{i+1} = g_{i+1} + \Delta u_{r_{i+1}} + u_{r_i} - \Delta \tag{36}$$

In matrix form this may be written as

Write equations Eq. (32), (33) and (34) in matrix form,

$$\begin{bmatrix} \overline{K} & -\overline{K} & 0 \\ -\overline{K} & \overline{K} & 0 \\ 0 & 0 & K \end{bmatrix} \begin{Bmatrix} \widehat{\Delta U} \\ \widecheck{\Delta U} \\ y_{u_r} \end{Bmatrix} + \begin{Bmatrix} \overline{Q} \\ -\overline{Q} \\ 0 \end{Bmatrix} = \begin{bmatrix} 1 & 0 & 0 & 0 & 1 \\ 0 & 1 & 0 & 0 & -\mu \\ 0 & 0 & 1 & 0 & -1 \\ 0 & 0 & 0 & 1 & -\mu \\ 0 & 0 & 0 & 0 & 1 \end{bmatrix} \begin{Bmatrix} \widehat{S}_r \\ \widecheck{S}_r \\ F_{c_r} \end{Bmatrix}$$
(38)

After some rearrangement we may obtain

$$\begin{Bmatrix} \hat{S}_r \\ \check{S}_r \\ F_{c_r} \end{Bmatrix} - \left[ \overline{K_n} \right] \begin{Bmatrix} \widehat{\Delta U} \\ \widecheck{\Delta U} \\ g_{q_r} \end{Bmatrix} = \left\{ \overline{Q_n} \right\}$$
(39)

Equation Eq. (39) along with conditions in Eqs. (23) and (27) are the LCP. It was proven by Sha et al. [6] that a unique solution exists and can be found if coefficient matrix is positive definite or positive semi-definite. Here matrix  $[\overline{K_n}]$  is a positive semi-definite matrix.

### 3. Examples

In the first example a simply supported beam under a uniform load shown in Figure 3 is studied. The beam is subjected to unilateral constraints at the midspan without friction. The beam is modelled using 19 three-node finite elements. A uniformly distributed load of 400 N/m is applied suddenly at time t = 0. Results up to 0.1 seconds are obtained using the proposed method with a time step of 0.1 ms. All other geometric and material properties are same as the second example. Figure 4 represents the results for both 15 and 20 mm of initial gap. Good agreement with Xu et al. [3] has been observed.

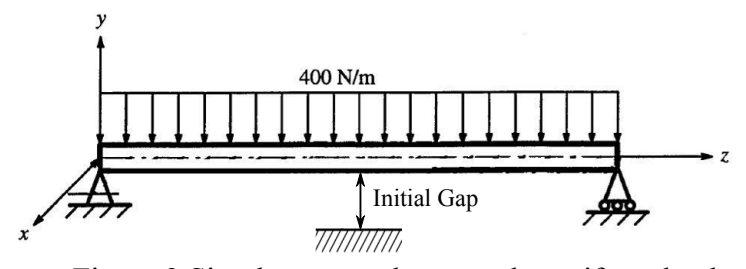


Figure 3 Simply support beam under uniform load

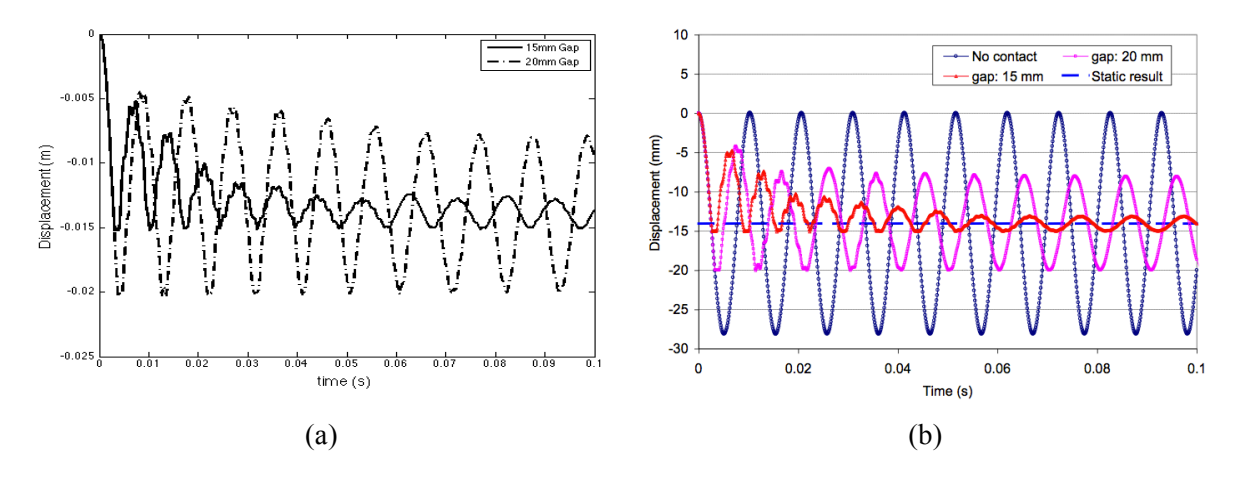


Figure 4 Displacement of the mid point (a) this paper, (b) Reference [3]

Xu et al. implemented Wilson  $\theta$  integration scheme in order to find the dynamic response of the rod. Scheme presented by Xu et al. can only model the unilateral contact without friction. Model presented in this paper is developed using Newmark integration scheme and will handle several unilateral contact subjected to two-dimensional contact.

In the second example a beam at 6 o'clock position with the clamped-clamped boundary conditions is studied. No structural damping is considered. The following harmonic excitations are applied to the centre of the beam in the three coordinate directions as shown in Figure 5,

 $Q_u = 5\cos(\omega_u t)$ ,  $Q_v = -15\cos(\omega_v t)$  and  $Q_w = 8\cos(\omega_w t)$  where  $\omega_v = 0.5 \, rad/sec$  and  $\omega_u = \omega_w = 5 \, rad/sec$ . Harmonic excitation is plotted in *Figure 6* (a) and (b).

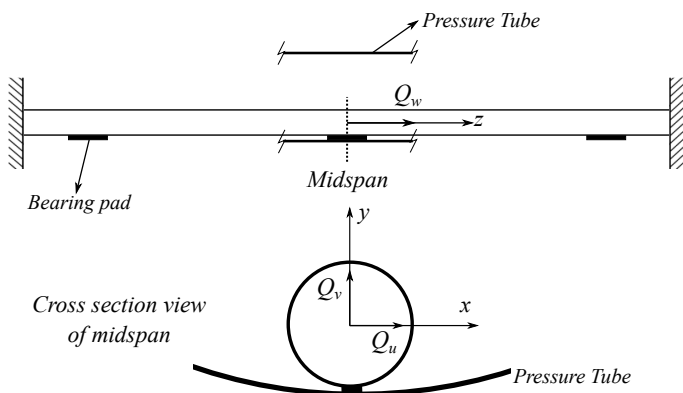


Figure 5 Three external excitation applied at the centre of the rod

Local contact stiffness and coefficient of friction are chosen as  $K = 1.0E8 \, N/m$ ,  $\mu = 0.5$  respectively, and all geometric and material properties are given below:

Length of fuel element L=0.5, Outside diameter of fuel element  $D_o=0.01308$ , Inside diameter of fuel element  $D_i=0.01228$ , Inside diameter of pressure tube  $D_{PT}=0.103$ , Thickness of bearing pads t=0.00145, Length of bearing pads  $L_{bp}=0.0254$ , Location of first bearing pad  $l_1=0.0445$ , Location of second bearing pad  $l_2=0.24765$ , Location of third bearing pad  $l_3=0.45080$ , Initial gap between fuel element and PT  $\Delta=0$ , Young's modulus E=80e9, Shear modulus G=26.2e9, Density of fuel element  $\rho=7850$ .

Figure 6 (c) and (d) shows the lateral, axial and torsional displacements of the beam at the midspan; Figure 7 shows the normal contact forces. The fuel element is modelled using 19 higher order finite elements. We did not consider the effect of pellets in this example and fuel element modelled as a hollow tube. One point of contact considered at the middle of central bearing pad. Three sinusoidal excitations applied at the midspan as mentioned before. The response was obtained for 20 seconds with a time step of 5 ms. The external excitation in the y direction had been given a low frequency  $\omega_v = 0.5 \text{ rad/s}$ , compared to the bending and axial excitations with an excitation frequency of 5 rad/s. With the procedure presented in this paper, the frictional forces handled as a two-dimensional friction successfully. As it can be seen from Figure 6 (c) and (d), sliding and stiction motion of the point of contact at the midspan observed in both bending and axial displacement. For the first period of the motion contact occurs from t = 0 till approximately  $t = 6.1 \, sec$  when fuel element separate from the pressure tube. In each period of time that contact happens damping in sliding motion due to friction can be seen from Figure 6 (c) and (d) in both axial and lateral displacements.

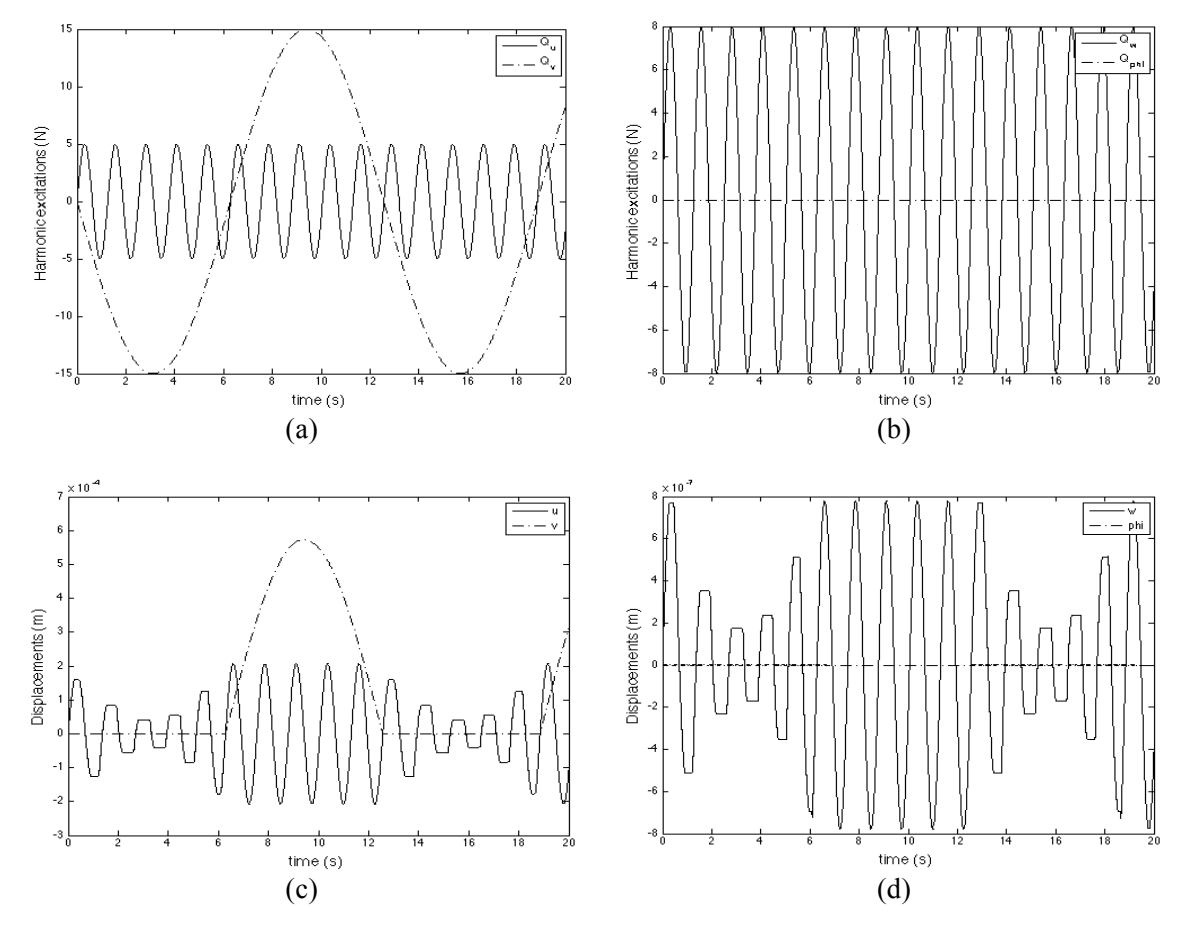


Figure 6 (a) Harmonic excitations in x and y directions, (b) Axial and torsional harmonic excitations (c) Lateral displacement in in x and y directions, (d) axial and torsional displacements

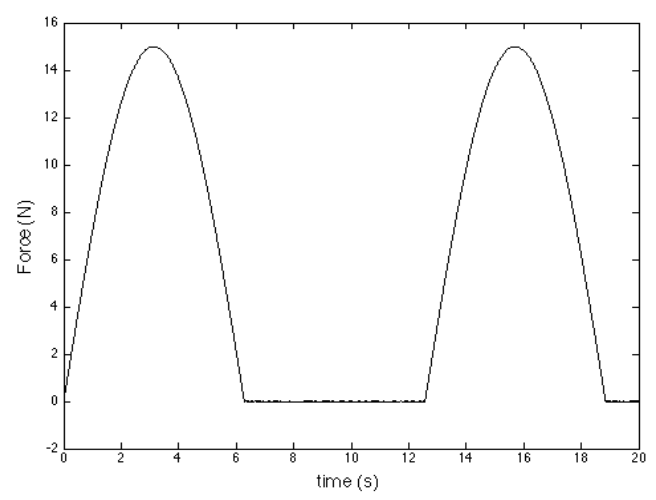


Figure 7 Normal contact forces

Small torsional dispalacment that observed in Figure 6 (d) is the result of coupling between lateral and torsional displacement due to presences of bearing pads.; *Figure 7* shows the normal contact forces for this particular example. It can be seen that the magnitude of the normal force increases and then decreases during the contact period due to the external excitation in the Y direction. These contact forces can be used to find the wear rate at the point of contact.

#### 4. Conclusion

The Bozzak-Newmark relaxation-integration scheme implemented successfully to discretize the equations of motion in the time domain for a single fuel element subjected to unilateral contact and 2D frictional constraints. Through a variable transformation, contacts and their associated frictional forces, the state of the system subjected to non-smooth constraints are reduced to a LCP for which a solution may be obtained using the Lemke algorithm.

To model CANDU fuel bundle vibration, the proposed procedure is being implemented into a computer code for modeling unilateral frictional contact between fuel elements through spacer pads and also between fuel bundle and pressure tube through bearing pads.

#### Acknowledgement

The authors acknowledge with appreciation the financial support from NSERC and SNC Lavalin Nuclear through a collaborative research grant.

#### 5. References

- [1] Yetisir, M., Fisher, N.J., "Prediction of pressure tube fretting-wear damage due to fuel vibration" Nuclear Engineering and Design. 1997. 176, 261–271.
- [2] Hassan, M., Rogers, R., "Friction modelling of preloaded tube contact dynamics. Nuclear Engineering and Design" 2005. 235, 2349–2357.

- [3] Xu S., Kim. Y. and Xu Z. "Modeling of Transient Dynamic Bundle Deormation Using Time Integration Scheme" 11<sup>th</sup> International Conference on CANDU Fuel, Niagra falls, Ontario, Canada, 2010 October 17-20.
- [4] S. D. Yu and M. Fadaee, "Comprehensive Dynamic Model for Axial, Flexural and Torsional Vibration of a CANDU Fuel Element" <u>Civil-Comp Press/Proceedings of the 11th International Conference on Engineering Computational Technology</u>, paper 297, 2012.
- [5] Yu S. D. and Hojatie. H. "Modeling lateral contact constraint among CANDU fuel rods" Nuclear Engineering and Design, 2012, 254 (2013) 16–22.
- [6] Sha D, Sun H, Zhang Z, et al. "A variational inequality principle in solid mechanics and application in physic- ally non-linear problems" Commun Appl Numer Methods 1990; 6: 35–45.